

Electronic supplementary information (ESI)

Porous materials based on organic macrocyclic molecules synthesized by Schiff-base chemistry for adsorption of iodine

Jiali Wen,^a Yi Lu,^a Fang Yang,^b Panli Sun,^{*b} Shaoqing Luo^c and Zongxia Guo^{*a}

^a College of Chemistry and Molecular Engineering, Qingdao University of Science and Technology, Qingdao 266042, PR China, E-mail: zxguo@qust.edu.cn

^b School of Polymer Science and Engineering, Qingdao University of Science and Technology, Qingdao 266042, PR China, E-mail: panlisun2017@163.com

^c Sharon High School, 181 Pond St, Sharon, MA 02067, United States

CONTENT

Experiments

1. Materials and instruments
2. Synthesis of OMM-1 and OMM-2
3. Iodine adsorption and desorption

Supplementary Figures (S1-S12)

Fig. S1 Solid-state ¹³C CP/MAS NMR spectrum of OMM-2

Fig. S2 HRMS spectrum of OMM-1

Fig. S3 HRMS spectrum of OMM-2

Fig. S4 TGA spectra of OMM-1 and OMM-2

Fig. S5 TEM images of OMM-1

Fig. S6 SEM and TEM images of OMM-2

Fig. S7 PXRD spectra of OMM-1 and OMM-2

Fig. S8 Pore-size distribution of OMM-1 and OMM-2

Fig. S9 Iodine vapor adsorption of OMM-1 at 75 °C under ambient pressure

Fig. S10 XPS spectra of OMM-1

Fig. S11 XPS spectra of I₂@OMM-1

Fig. S12 PXRD spectra of I₂@OMM-1 and regenerated OMM-1 powders

Fig. S13 ATR-FT-IR spectrum of regenerated OMM-1 powder

Supplementary tables (Table S1-S2)

Table S1. Porosity parameters of the OMMs

Table S2. Summary of iodine uptake capacity for some of the reported porous adsorbents

Experiments

1. Materials and instruments

1,8-diaminoanthracene are synthesized according to literature. Terephthalaldehyde (reagent grade) and m-Phthalaldehyde (reagent grade) were purchased from Energy Chemical. Mesitylene (reagent grade), 1,4-dioxane (reagent grade), Acetic Acid (AcOH, reagent grade), tetrahydrofuran (reagent grade, THF) and acetone (reagent grade) were purchased from Sigma-Aldrich Corporation. The solvent THF and acetone were dried under conventional methods. Unless otherwise noted, the chemicals were used as received.

The Element Analysis was performed on a Vario EL III element analyzer (Elementar, Germany) by using the operation mode of CHN. The purities of OMMs are calculated by $\frac{C\%_{\text{experimental}}}{C\%_{\text{theoretical}}} \times 100\%$, $\frac{H\%_{\text{experimental}}}{H\%_{\text{theoretical}}} \times 100\%$, and $\frac{N\%_{\text{experimental}}}{N\%_{\text{theoretical}}} \times 100\%$, respectively. The minimum calculated value among three elements was selected as the reasonable purity for each OMM. Scanning electron microscopy (SEM) was carried out using a FEI Quanta FEG 250 scanning electron microscopes, samples were dispersed in ethanol then dropped 0.8 μL on a mica plate over a slice of conductive adhesive which adhered to a sample holder, and then coated with Pt using a sputter coater sputtered for 60 s before SEM measurement. The sample preparation methods for Energy Dispersive X-Ray (EDX) were identical with SEM. Transmission electron microscopy (TEM) was conducted on a FEI TECNAI 20 operating at 190 kV, samples for TEM were dispersed in ethanol then dropped on copper grids covered with carbon film until the solvent was evaporated. Fourier transform infrared spectroscopy was carried out with a BRUKER HQL005 FTIR spectrometer and Bruker Tensor 27 in the 400-4000 cm^{-1} region by using the Attenuated Total Reflection (ATR). Solid-state ^{13}C NMR cross polarization (CP) spectra was performed on Agilent 600 DD2 spectrometer at a resonance frequency of 150.45 MHz. ^{13}C CP/MAS NMR spectra was recorded with spinning rate of 15k Hz with a 4 mm probe at room temperature with a delay time of 3 s and a contact time of 2 ms. Mass spectral data were obtained by using a DCTB matrix-assisted laser desorption/ionization time of flight mass spectrometry (MALDI-TOF MS) instrument. Powder X-ray diffraction (PXRD) measurement was performed on a Bruker D8 Advance diffractometer using Cu K α radiation over the range of 5-60 $^{\circ}$. Thermal gravimetric analyses (TGA) was carried out on a TA Q20 by heating the samples from 30 to 800 $^{\circ}\text{C}$ under nitrogen atmosphere at a heating rate of 10 $^{\circ}\text{C min}^{-1}$, samples were degassed at 120 $^{\circ}\text{C}$ for 1 h under vacuum before analysis. The surface areas and pore size distributions were determined using ASAP 2420 accelerated surface area and porosimetry system (Micromeritics Instrument Corporation, USA) by nitrogen adsorption and desorption at 77 K, samples were degassed at 120 $^{\circ}\text{C}$ for 10 h under vacuum before measurement.

2. Synthesis of OMM-1 and OMM-2

2.1 Synthesis of OMM-1

A mixture of 1,8-diaminoanthracene (41.6 mg, 0.2 mmol) and terephthalaldehyde (26.8 mg, 0.2 mmol) was placed into 300 mL Parr 4560 Mini pressure reactor, after that the mixture of mesitylene/1,4-dioxane/6M AcOH (19/1/2 by vol., 11 mL) was added into reactor smoothly. After reactor degassed by three freeze-pump-thaw cycles and purged with nitrogen, the reactor was heated up to 120 °C and remained for 72 h without any disturbance. Then the system was cooled to room temperature and the product was collected by centrifugation. After washed with anhydrous tetrahydrofuran (THF) and acetone and dried under dynamic vacuum at 120 °C for 10 h, the product was collected as a brick red powder (53 mg, 86%). The theoretical content of C, H, N are 86.25%, 4.61% and 9.14% for OMM-1. The experimental content of C, H, N were 87.87%, 5.30% and 8.79% based on element analysis. Then the calculated purity of OMM-1 in powder was 96.13%.

2.2 Synthesis of OMM-2

A mixture of 1,8-diaminoanthracene (62.4 mg, 0.3 mmol) and m-Phthalaldehyde (40.2 mg, 0.3 mmol) was added to a heavy-wall pressure reactor, then a mixture of mesitylene/1,4-dioxane/6M AcOH (19/1/2 by vol., 16.5 mL) was added. Next, the reactor was degassed by three freeze-pump-thaw cycles and purged with nitrogen. The reactor was sealed and heated at 120 °C for 3 days under undisturbed condition, when the system was cooled to room temperature, the product was collected by centrifugation, washed with anhydrous THF and acetone, and then dried under dynamic vacuum at 120 °C for 10 hours to afford a yellow powder (92 mg, 83%). The theoretical content of C, H, N are 86.25%, 4.61% and 9.14% for OMM-2. The experimental content of C, H, N were 84.53%, 5.12% and 8.70% based on element analysis. Then the calculated purity of OMM-2 in powder was 95.19%.

3. Iodine adsorption and desorption

3.1 Iodine vapor adsorption experiment procedures

Firstly, the OMM powder and excess iodine were placed in sealed containers at 75 °C under ambient pressure. After that, the sample weight before and after iodine vapor adsorption was compared by gravimetric analysis to determine the iodine enrichment of OMMs.

3.2 Iodine desorption experiment procedures

Iodine desorption experiment was performed as follows: I₂@OMM-1 was put in a heat-resistant bottle and heated at 125 °C under ambient pressure. The release efficiency was calculated by $(m_0 - m_t)/m_t \times 100\text{wt}\%$, where 'm_t' is the mass of the iodine trapped in I₂@OMM-1, 'm_t' is the mass of I₂@OMM-1 at a certain time, and 'm₀' is the initial mass of I₂@OMM-1 without heat at the beginning.

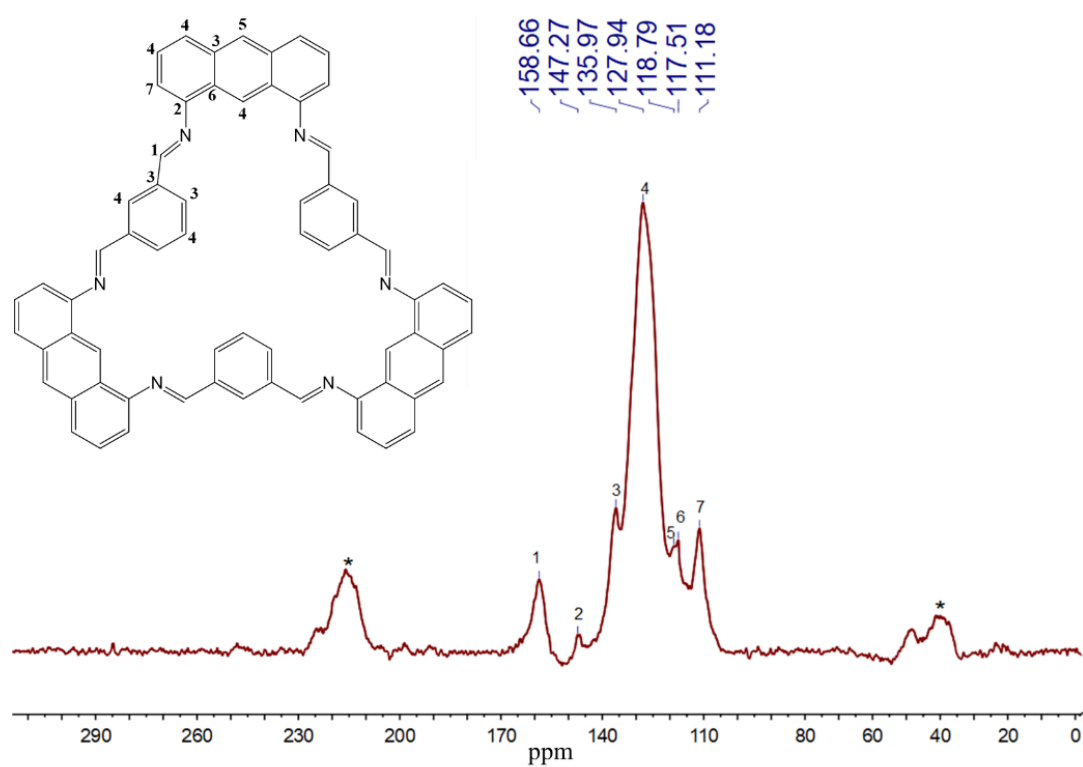


Fig. S1 Solid-state ^{13}C CP/MAS NMR spectrum of OMM-2.

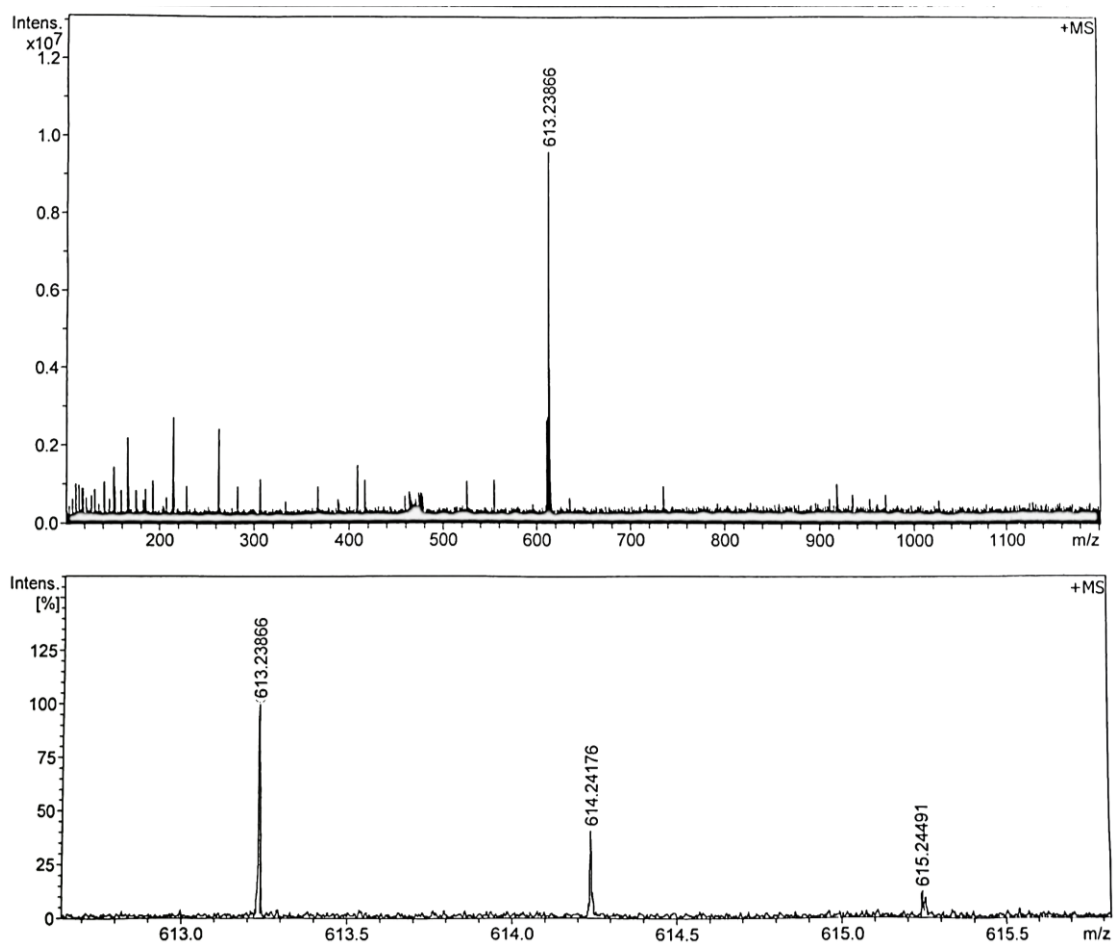


Fig. S2 HRMS spectrum of OMM-1.

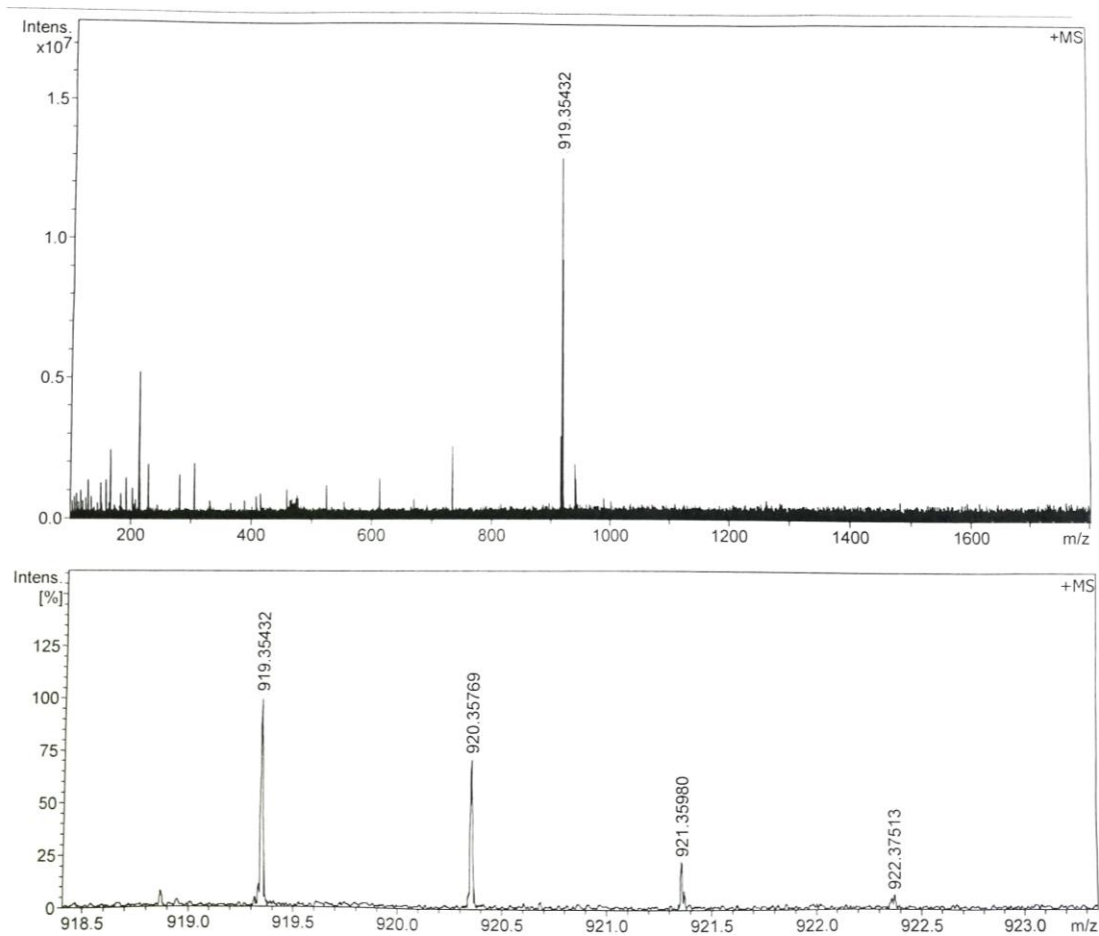


Fig. S3 HRMS spectrum of OMM-2.

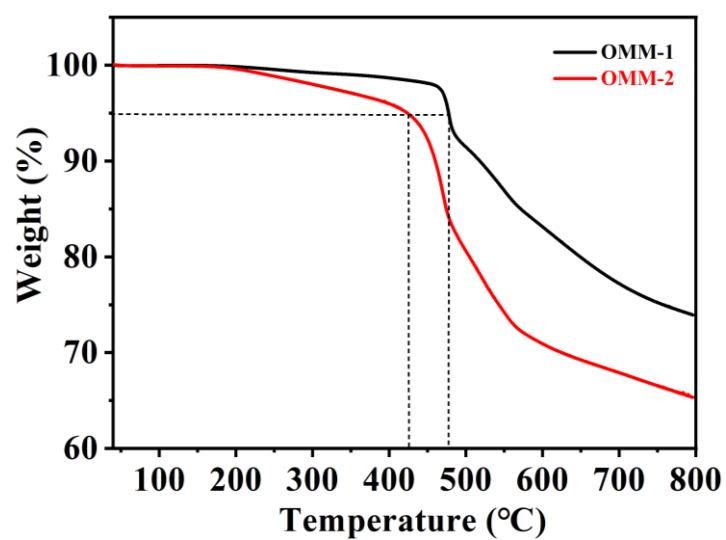


Fig. S4 TGA spectra of OMM-1 and OMM-2.

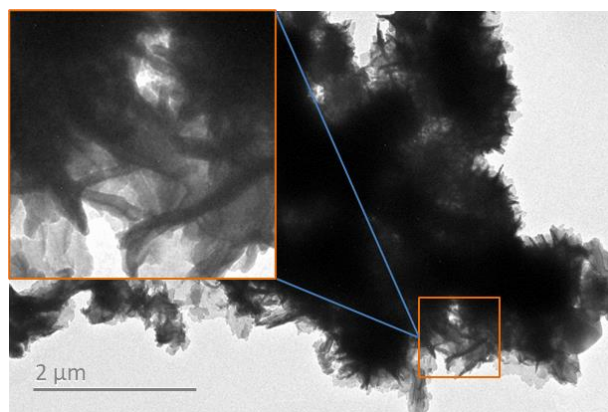


Fig. S5 TEM images of OMM-1.

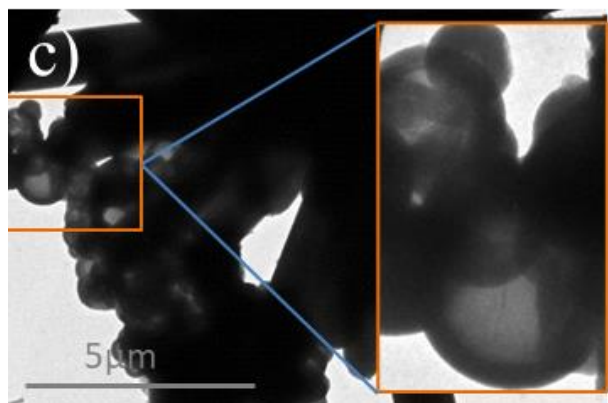
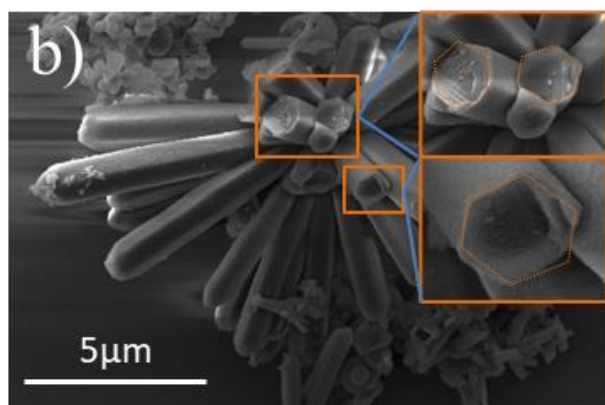
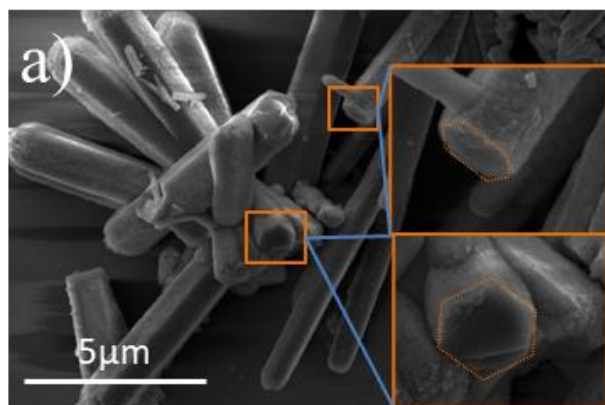


Fig. S6 SEM and TEM images of OMM-2.

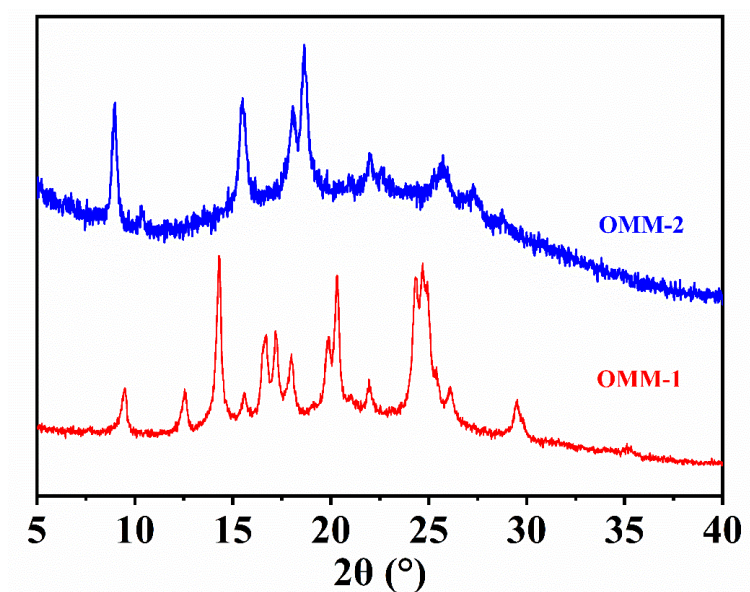


Fig. S7 PXRD spectra of OMM-1 and OMM-2.

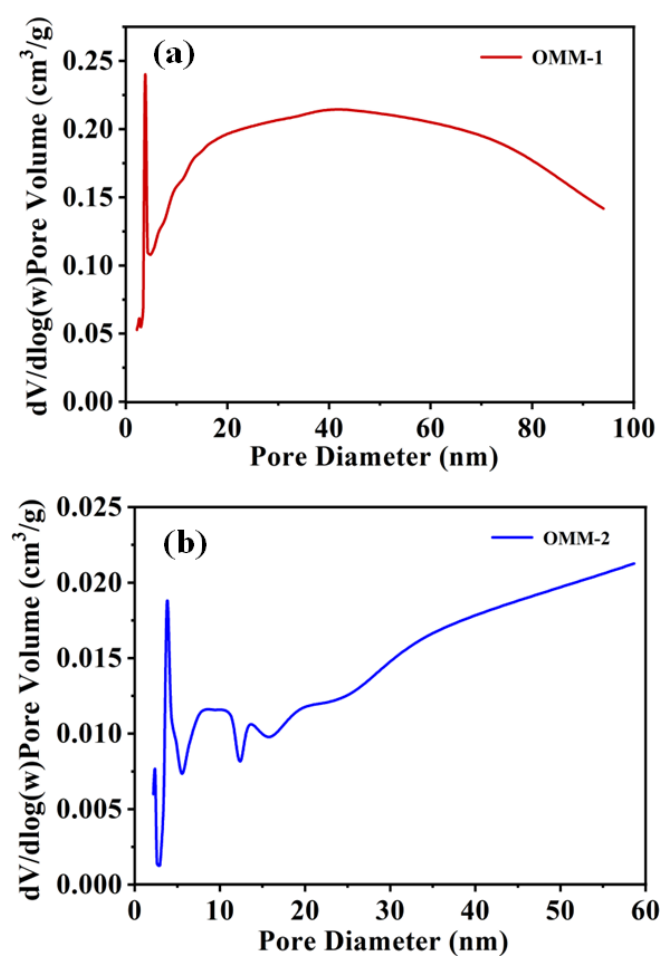


Fig. S8 Pore-size distribution of OMM-1 and OMM-2.

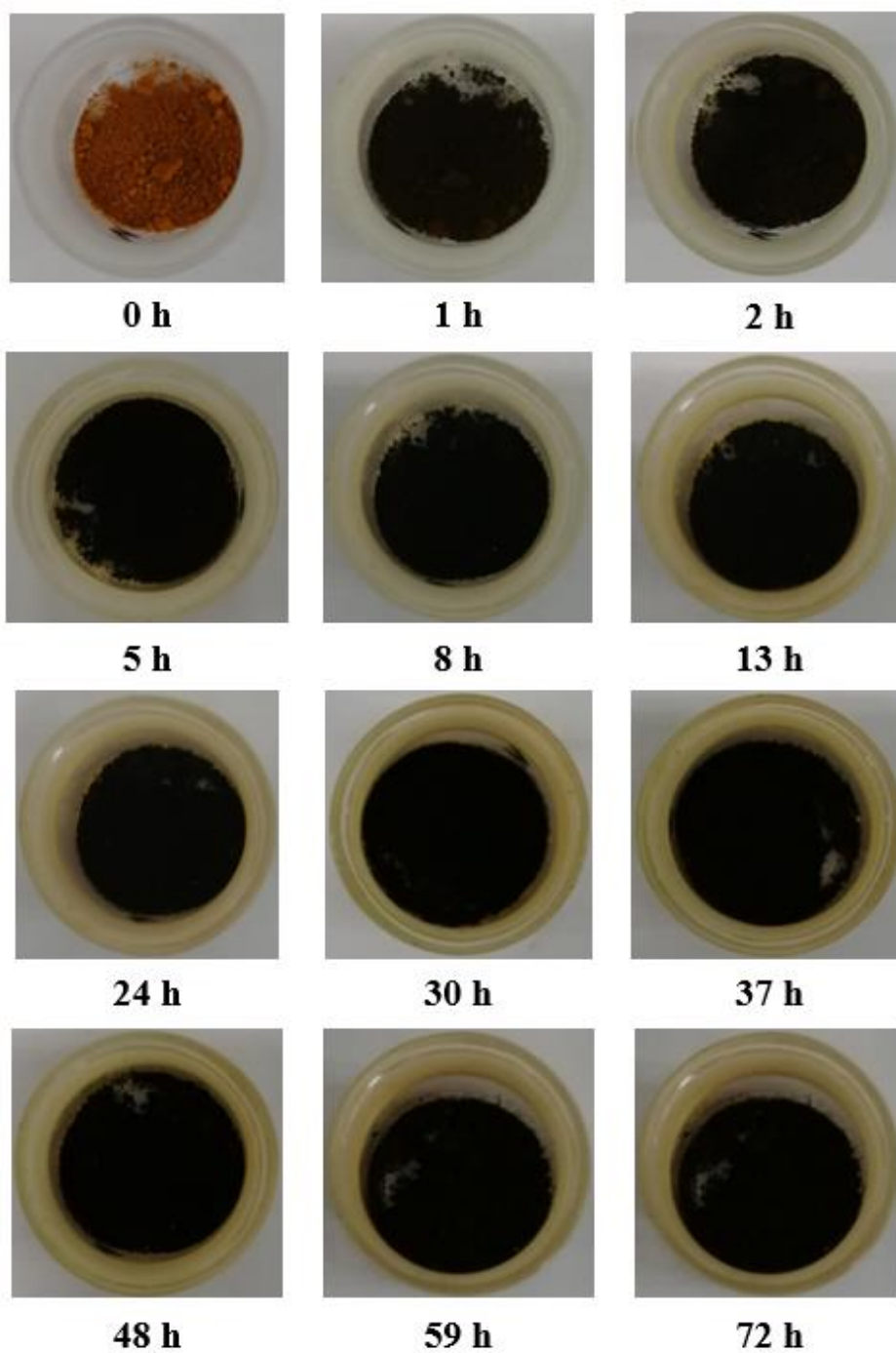


Fig. S9 Iodine vapor adsorption of OMM-1 at 75 °C under ambient pressure.

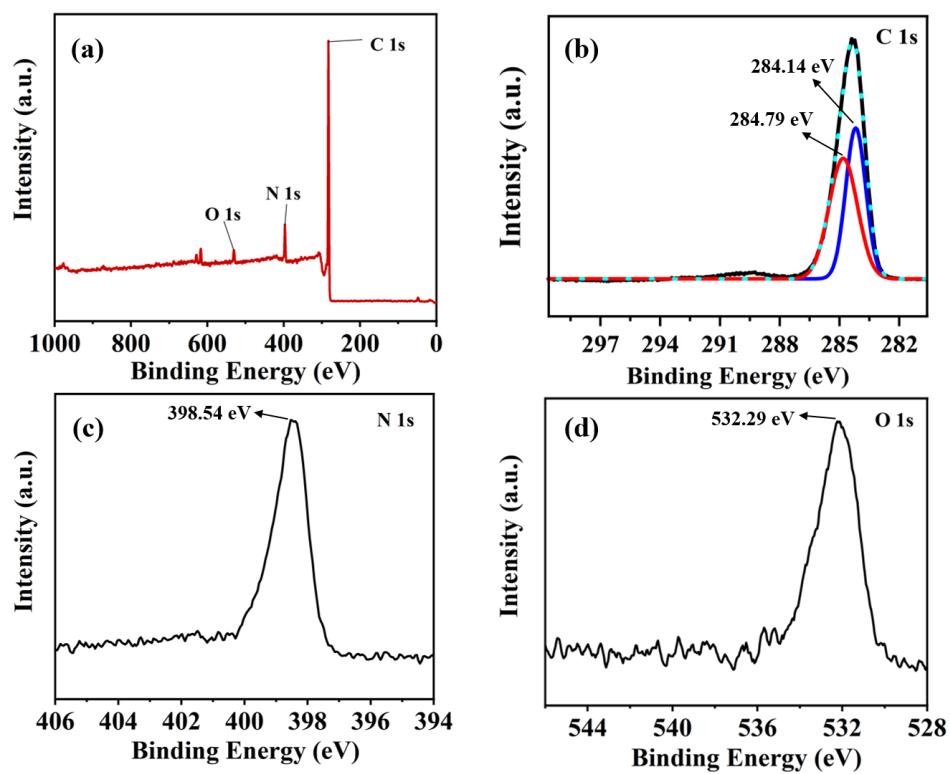


Fig. S10 XPS spectra of OMM-1.

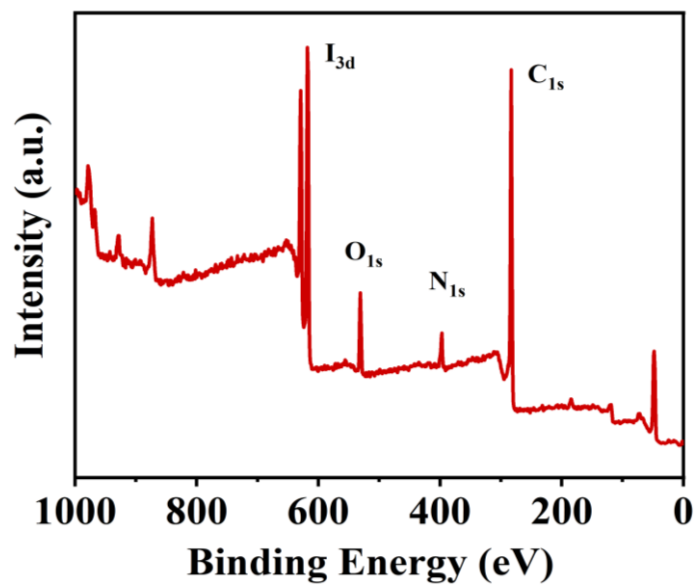


Fig. S11 XPS spectra of I₂@OMM-1.

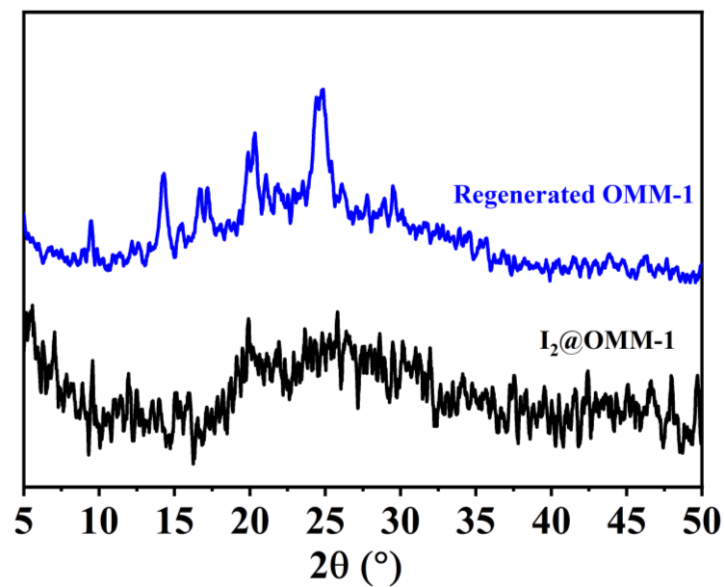


Fig. S12. PXRD spectra of $I_2@OMM-1$ and regenerated OMM-1 powders.

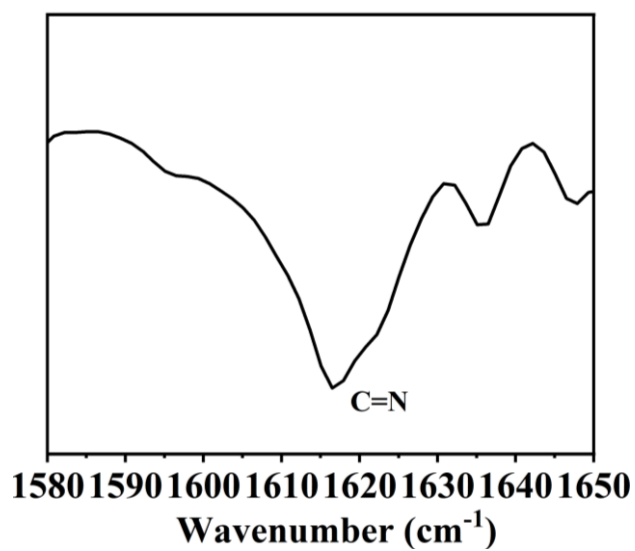


Fig. S13 ATR-FT-IR spectrum of regenerated OMM-1 powder.

Table S1. Porosity parameters of the OMMs.

Materials	S_{BET} ($\text{m}^2\cdot\text{g}^{-1}$)	S_{micro} ($\text{m}^2\text{ g}^{-1}$)	V_{total} ($\text{cm}^3\text{ g}^{-1}$)	D_{pore} (nm)
OMM-1	95.97	-	0.23	11.60
OMM-2	11.53	1.76	0.03	11.05

Table S2. Summary of iodine uptake capacity for some of the reported porous adsorbents.

Adsorbent	I_2 uptake (g g^{-1})	reference
BisImi-POP@2 ^a	10.30	ACS Applied Polymer Materials 2020, 3, 354-361
iCOF-AB-50 ^b	10.21	ACS Macro Letters 2021, 10, 12, 1590-1596
TBIM ^a	9.43	Journal of Materials Chemistry A 2020, 8, 2820-2826
iCOF-AB-33 ^b	9.00	ACS Macro Letters 2021, 10, 12, 1590-1596
IL@PCN-333(Al) ^c	7.35	Journal of Materials Chemistry A 2019, 7, 18324-18329.
NR_POP-C2 ^a	7.16	ACS Appl. Polym. Mater. 2024, 6, 7368-7382
TPDA-TFPB CMP ^a	6.48	Molecules 2024, 29, 2242
SR-KOH ^d	6.46	Chemical Engineering Journal 2019, 372, 65-73
MPOP-4 ^a	6.30	Chemical Engineering Journal 2024, 498, 154894
60PEI@HCP ^a	6.07	Journal of the Taiwan Institute of Chemical Engineers 2018, 93, 660-666
SCU-COF-2 ^b	6.00	Chem 2021, 7, 699-714
HBTZ ^a	5.66	Polymers for Advanced Technologies 2023, 34, 1529-1539
BPPOC	5.64	Journal of the American Chemical Society 2022, 144, 12390-12399
TJNU-201 ^b	5.62	Journal of Materials Chemistry A 2020, 8, 9523-9527
NR_COFC-1 ^b	5.45	J. Mater. Chem. A, 2024, 12, 10539-10553
HKUST-1@PES ^c	5.38	Advanced Functional Materials 2018, 28, 1801596.
CMP-LS8 ^a	5.29	Journal of Hazardous Materials 2020, 387, 121949-121958.
BID[3]s^e	5.12	CCS Chemistry 2022, 4, 1806-1814
TTPA ^a	4.92	Microporous and Mesoporous Materials 2019, 273, 163-170
SIOC-COF-7 ^b	4.81	Chemical Communications 2017, 53, 7266-7269
COF-DL229 ^b	4.70	Chemistry-A European Journal 2018, 24, 585-589
HPDA ^b	4.53	Journal of Applied Polymer Science 2022, 139, 37, e52889
NDB-H	4.43	Chemistry-An Asian Journal 2018, 13, 2046-2053
CMP-LS5 ^a	4.4	Polymer Chemistry 2019, 10, 2608-2615
PCN-333(Al) ^c	4.42	Journal of Materials Chemistry A 2019, 7, 18324-18329
NDB-S	4.25	Chemistry-An Asian Journal 2018, 13, 2046-2053
OMM-1^e	4.22	This work
TBAPB ^b	4.13	Reactive and Functional Polymers 2023, 184, 105516
PG-800 ^a	4.11	Chemistry Select 2018, 3, 10147-10152
PHF-1-Ct ^a	4.05	Chemical Communications 2018, 54, 12706-12709
tCTF-Cl-3	3.48	Journal of Polymer Research 2022, 29, 153
OMM-2^e	3.74	This work
PHF-1 ^a	3.05	Chemical Communications 2018, 54, 12706-12709
CTF-CTTD-500 ^a	3.87	Industrial & Engineering Chemistry Research 2018, 57, 15114-15121
OMM-2	3.74	This work
ADB-HS	3.45	Chemistry-An Asian Journal 2018, 13, 2046-2053

ADB-S	3.42	Chemistry-An Asian Journal 2018, 13. 2046-2053
HCMP-3 ^a	3.36	Macromolecules 2016, 49, 6322-6333.
NRPOP-2 ^a	3.17	Scientific Reports 2022, 12, 2638.
PTPATTh ^a	3.13	Journal of Solid State Chemistry 2018, 265, 85-91
CalP4-Li ^a	3.12	Chemistry of Materials 2017, 29, 8968-8972
CMP@3	3.08	Chemistry Select 2022, 7, e202200234
Cu _{0.25} Pc-COF ^b	2.99	Chinese Chemical Letters 2022, 33, 3549-3555
DDHP-COF ^b	3.0	Chinese Chemical Letters 2023, 34, 4, 107454
AzoPPN ^a	2.9	Chemistry-A European Journal 2016, 22, 11863-11868
BDP-CPP-1 ^a	2.83	Journal of Materials Chemistry A 2017, 5, 6622-6629.
PAF-24 ^a	2.76	Angewandte Chemie International Edition 2015, 54, 12733-12737
COF-TpgDB ^b	2.60	ACS Omega. 2020, 5, 24262
TPBTz	2.49	Journal of Porous Materials 2020, 29, 5, 15665-1573
TpPa-1	2.45	Journal of solid state chemistry, 2019, 279, 120979-120979
CMP-LS6	2.44	Polymer Chemistry 2019, 10, 2608.
Azo-Trip ^a	2.38	Polymer Chemistry 2016, 7, 643
Uassis-PC800	2.25	Chemical Engineering Journal 2020, 382, 122997
CalP4 ^a	2.20	Chemistry of Materials 2017, 29, 8968-8972
MOF-808 ^c	2.18	ACS Applied Materials & Interfaces 2020, 12, 20429-20439
BN foam	2.12	Chemical Engineering Journal 2020, 382, 122833
MALP-1	2.09	Industrial & Engineering Chemistry Research 2019, 58, 17369
Azo-POP1 ^a	1.57	Polymer 2025, 317, 127873
AIOC-155	0.86	Inorganic Chemistry Frontiers 2022
UiO-66-NH2@WCA	0.704	Journal of Hazardous Materials 2023, 443, 130236
Bi/Cu-BTC@g-C3N4	0.588	Separation and Purification Technology 2025, 354, 128746
CTF-Cl-4 ^a	0.58	Chemistry-An Asian Journal 2019, 14, 3259-3263
EtP6β	0.2	Journal of the American Chemical Society 2017, 139(43), 15320-15323
N ₄ O ₄ ^c	0.2	Microporous & Mesoporous Materials 2016, 226, 53-60

^aPOPs, ^bCOFs, ^cMOFs, ^dPorous Carbon, ^eorganic macrocyclic molecule